Characterizing Release in Electrospun PCL Capsules: Preliminary Findings for Future Model Design

Undergraduate Thesis

Presented in partial fulfillment of the requirements for the degree
Bachelor of Science with Honors Research Distinction.

By

Kaden L. Zachmann

Undergraduate Program in the Department of Biomedical Engineering

The Ohio State University

2017

Committee:

John J. Lannutti, Advisor

Katelyn E. Swindle-Reilly

Abstract

Engineering controlled drug release is a biomedical research interest due to its many clinical applications including: disease targeting, sustained release, and eliminating the need for repeating dosages. For example, in veterinary medicine, there is a need for a long-lasting and reversible contraceptive option for large and small animals. A device made of electrospun material is proposed to provide longer lasting release of Deslorelin, gonadotropin-releasing hormone agonist than current conceptive devices. Engineering this capsule-based device requires an understanding of the polymer components, one of which will be a layer of electrospun polycaprolactone (PCL). The short-term release of a specific fluorescent dye, Rose Bengal, through a single layer of sintered electrospun PCL was quantified in two solutions: distilled water and phosphate buffered saline (PBS). The results showed that the PBS solution significantly ($p=0.0006$) impacted the release of the dye. PBS induced an average flux of 0.009 ng/mm^2-day while the flux in solution without PBS was essentially nil. These results prompted further investigation and a literature review of available drug release models to create a better understanding of the plausible mechanisms of release. The implication of this investigation is that diffusion may not be the only significant contributor to the release through these capsules, as is often assumed.

Acknowledgments

I would like to thank The Ohio State University College of Engineering for the research scholarship and opportunity to publish this undergraduate thesis. I would like to thank Dr. John J. Lannutti for providing the lab, resources, and support for this project. I would like to thank Francisco J. Chaparro for his training, guidance, and support for this project. I would like to thank Dr. Tyler M. Nelson for his training, guidance, and support while working in this lab.

Vita

June 2014 .....Pleasant High School Marion, OH

Fields of Study

Major Field: Biomedical Engineering

Table of Contents

List of Figures

List of Tables

Introduction

A. Significance of Drug Release

There is a significant need for improved drug eluting devices. Investigations into specific forms of such devices comprise a significant component of research within academia and industry. This is in part due to the complexities of biology and disease, and in part due to the regulatory and economic constraints associated with medical device design. First, the importance of drug delivery, and drug targeting is intuitive for: diseases such as cancer, localized infection sites, diagnostic imaging, and limiting the biofouling responses occurring at device interfaces. With precise control over the drug delivery, smaller yet clinically effective amounts of a potentially harmful drug (e.g., many chemotherapeutics) can be administered. Drug release is important for ensuring the drug's performance, improving patient compliance, and decreasing patient risk. Second, the regulatory pathways to developing a drug eluting mechanism are much simpler, faster, and less expensive than those associated with developing novel drugs. This allows new treatments to be developed quickly by effective modification of the delivery and use of already approved drugs.

Sustained drug release is a particular area of interest, especially for medicine in which patient compliance and dosing is important. For example, Figure 1 shows what the concentration of repeated regular dosing of a drug may look like, compared to a sustained release of the required concentration. There is also a narrow range for the concentration required for the drug to be therapeutic, and a level when the concentration would become toxic. The ideal sustained drug would allow the concentration of drug to

remain constant without peaks and valleys, such as the regular dosing, which can fluctuate near toxic levels especially in the case of medication misuse.

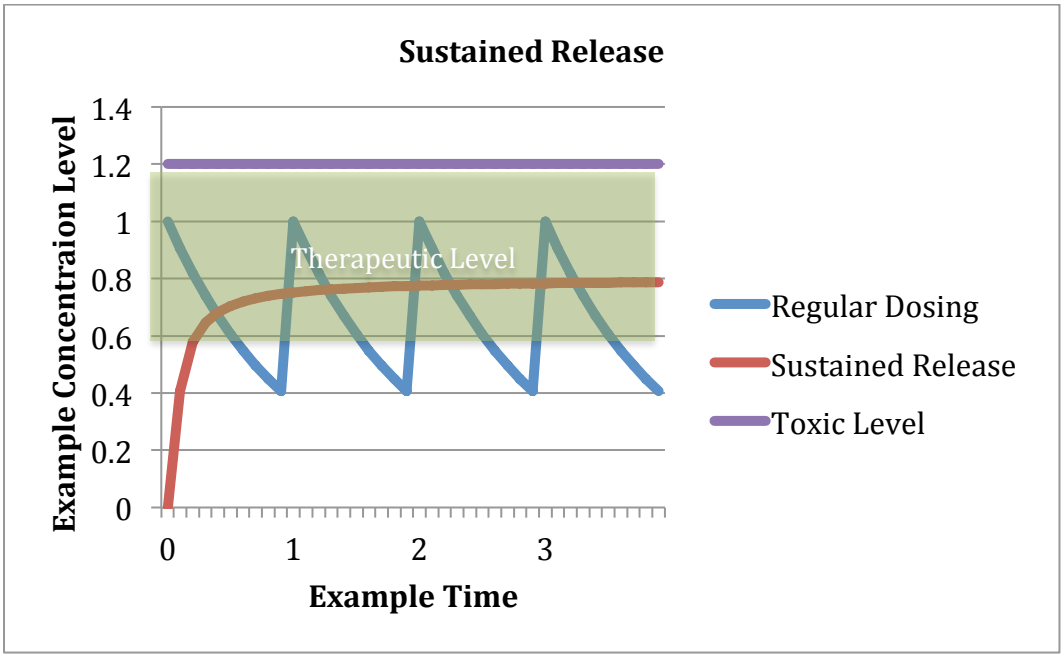

Figure 1. Benefits of sustained release vs. regular dosing

There are a variety of medications available, which utilize sustained release mechanisms. Oral medications can last for several hours, or be engineered to release at a specified time (hours) after consumption. But, there are also a few implantable medical devices available, which elute drugs. Probably the most common of these implants are used in contraceptive medicine. Implanon, a high efficacy product released in the US in 2006, is an implantable product available for females, which regulates the reproductive system hormonally. The implantable cylindrical device can be used for at most 3 years before it needs to be replaced[1]. The device is made of an ethylene-vinyl acetate layer which controls the steady release of etonogestril[1].

In veterinary sciences, there is an implant available for companion animals, as an alternative to irreversible surgeries or permanent treatments available only for young animals. Suprelorin, an implant, lasts just 1-2 years. However, there is an interest in finding a treatment for animals that will allow for both life-long contraception while still allowing the possibility of restoration of fertility [2-4].

B. Research Overview

By modifying the creation, structure, and layers of nanofiber capsules, it has been proposed that an implantable device can be created which will provide continuous release of appropriate drug concentrations for longer periods of time than current drug eluting implants. This device could specifically be used for the sustained release of appropriate levels of gonadotropin-releasing hormone (GnRH) agonist, Deslorelin, in companion animals as a long-term contraceptive option. This could offer a potential solution to many ethical issues surrounding animal overpopulation. The current research goal is to create a device lasting longer than 3 years.

In order to create a novel device with the appropriate effective period, a multi-layered approach will be utilized. A layered delivery vehicle will have: one layer (#3 on Figure 2) being a highly biomimetic outer layer that will be biodegradable and create minimal tissue irritation upon implantation, a second interior layer (#2 on Figure 2) being a nanofiber geometry that will allow for the appropriate diffusion rate of the drug, and Deslorelin suspended in oil, as the drug payload (#1 on Figure 2). The appropriate nanofiber layers, compositions, and release mechanisms are being determined and investigated through experimentation. The current method used for manufacturing nanofiber polymers, is electrospinning.

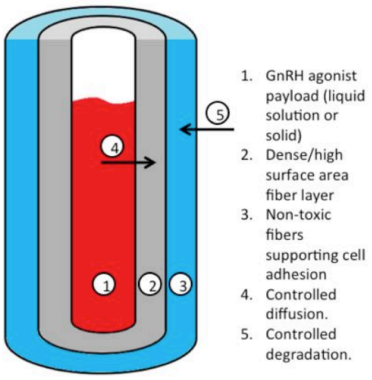

Figure 2. A layered multifunctional delivery vehicle design.

C. Electrospinning

Electrospinning is a method of manufacturing micro or nanoscaled diameter polymer strands. It can be used to create biomimetic, reproducible, and engineered nanofiber matrices (Figure 3). Electrospinning involves a dissolved polymer solution, high voltage supply, conductive capillary tube, and typically a conductive collecting surface (Figure 4).

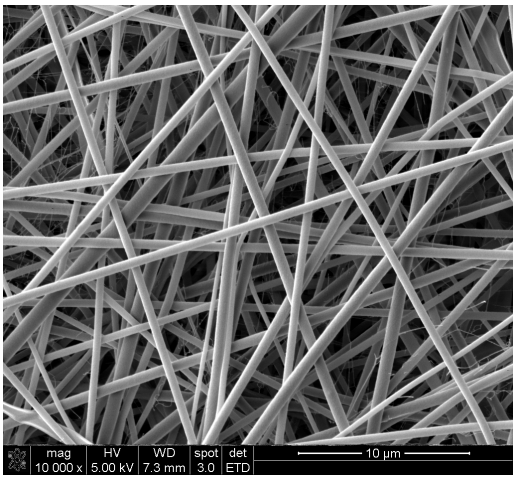

Figure 3. Scanning electron microscope image of electrospun nanofibers.

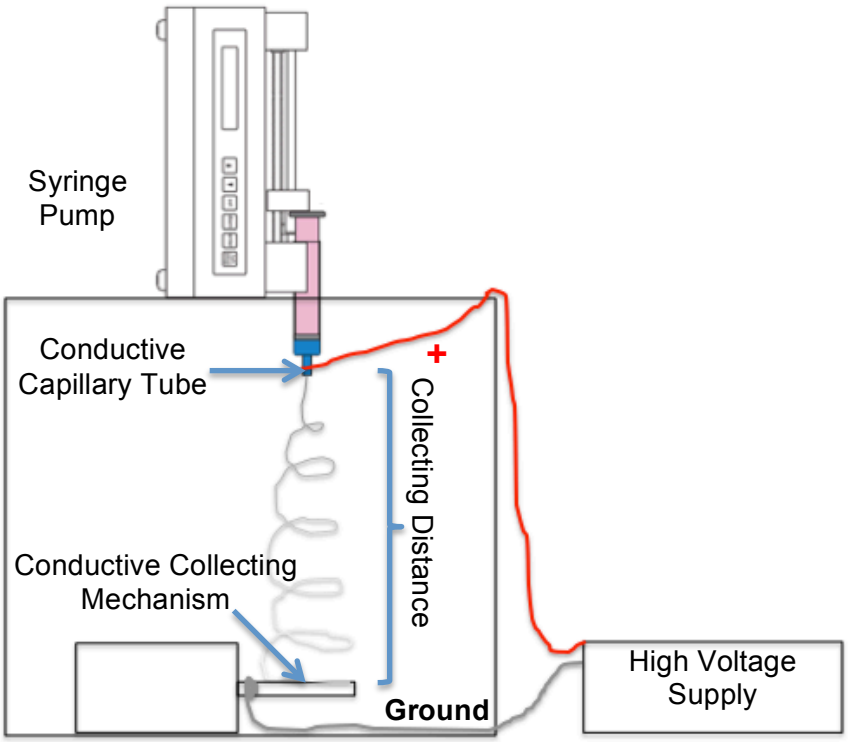

Figure 4. Schematic of an electrospinning setup.

The electric current applied to the polymer solution is integral to the electrospinning process. When the liquid is in the discharging capillary tube, a charge is induced on the surface of the liquid. Mutual charge repulsion and the resulting force opposite the surface tension induces the droplet extension (shown below in Figure 5) [5,6].

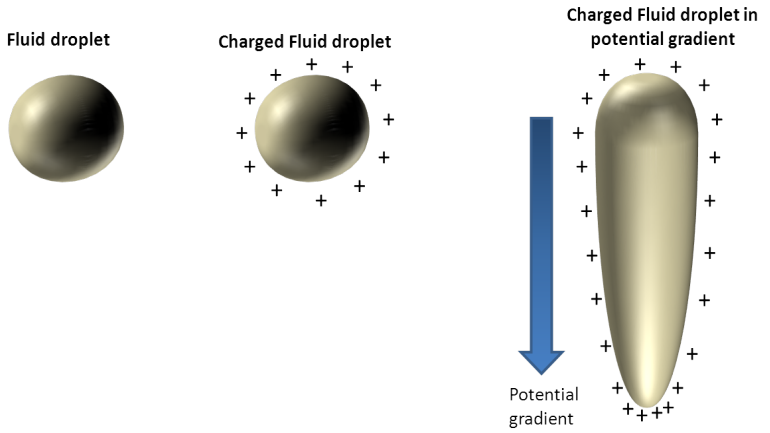

Figure 5. Mutual charge repulsion results in extension of particle surface area.

The extended droplet eventually forms a conical shape known as the Taylor Cone. As the force applied from the electrical current surpasses the force of the surface tension, a charged fluid is ejected from the tip of the Taylor Cone. The solution evaporates as the target polymer left behind elongates further. Due to the effects of mechanical whipping, the charged fiber extends as it moves towards the neutrally or oppositely charged collector, where it will settle and collect to form a matrix in its final, fully solidified polymeric state[5] (Figure 3).

Electrospinning setup parameters impact the resulting nanofiber matrix properties, and are advantageous for engineering unique materials. Some basic parameters, which can be easily manipulated, are described in Table 1, however, specific values for these parameters vary greatly based on the material and the application[7]. Although there are models that describe the overall effects of process conditions on fiber production, considerable experimentation is typically required to establish optimized versions of these parameters. And it should be noted that these parameters may impact one-another as they are changed. Electrospinning process such as emulsion spinning and

core-shell spinning are additional modifications that can be used to create novel materials.

Table 1. A tabular description of general electrospinning parameters.

Parameters:	Impact at Low:	Impact at Moderate or Threshold value:	Impact at High:	
Collecting Distance	At too low of a collecting distance, the solvent may not evaporate, resulting in non-uniform polymer matrices.	There is a minimum threshold distance that allows a clean collection of polymer strands without solvent.	As this distance is increased, it has been seen that fibers can be made thinner. As they thin, they are more likely to break.	
Applied Voltage	At too low of a voltage, the Taylor Cone will not form and will result in solution dripping.	There is a minimum voltage threshold that must be overcome for the Taylor Cone to form.	Higher voltages will continue to increase the charge repulsion of the droplet, impacting: fiber diameter and collection time.	Even higher voltages can cause multiple jet streams.
Collector Shape and Motion	If a collector is stationary slow or wide shaped, the fibers will collect in random orientation.	Large and narrow collectors with a high amount of surface area can be moved, and specifically spun, to achieve varying degrees of fiber alignment.	With high speeds and a large surface area, nearly completely aligned fibers can be generated.	
Flow Rate	With slower flow rates, thinner fibers have been made.		With faster flow rates, thicker fibers have been made.	
Solution Viscosity	With low solution viscosity, electrospraying (a process of generating sub-micron beads) is achieved.	With moderate viscosities, electrospinning results in thin fibers with large beads.	With high enough viscosity, smooth nanofibers are achieved.	Higher: thick fibers, or an un-spinnable solution
Polymer Concentration	With low concentrations, electrospraying is achieved.	With moderate concentrations, electrospinning results in thin fibers with large beads.	With high enough concentration, smooth nanofibers are achieved.	
Polymer molecular weight	With low molecular weight, electrospraying is achieved.	With moderate polymer weights, electrospinning results in thin fibers with large beads.	With high polymer molecular weight, smooth nanofibers are achieved.	Higher: thick fibers

D. Electrospinning Applications and Impact

Electrospinning has been used successfully in air and water filtration, tissue engineering, and regenerative medicine[5]. Its attention has grown over the past decades in research and development. This is largely due to an increased interest in nanotechnology, and the great amount of flexibility, high throughput, and low costs electrospinning offers [8]. The first commercial products based on sub-micron fibers were introduced in the early 1980s in the United States by Donaldson Co., Inc [8]. And there have been many more moves to commercialization since [6,8,9]. For example, electrospun materials have been used in a number of commercial air filtration applications due to better filter efficiency [8]. And since 2012, it has been shown that electrospun fiber can also be used for effective water filtration [10]. Several properties of electrospun matrices can account for its success in filtration: the matrix structure of interconnected open pores, high permeability for gases, and a large surface area per volume ratio [11].

Some specific electrospun materials have also received special interest because they have been found to be highly biocompatible[9,12,13]. The nanofibrous geometry of an electrospun matrix is similar to the extracellular matrix that exists *in vivo*, giving it biomimetic properties especially useful for tissue engineering, implant design, and cell migration studies[12]. And additionally, these properties make electrospun materials especially promising in the field drug delivery. There have been a variety of approaches to creating electrospun drug-eluting materials including: drug adsorption to nanofiber, drug carrying nanoparticle adsorption to nanofiber, electrospun blends, and electrospinning using a drug core[13].

E. Sintered Polycaprolactone (PCL)

One main approach used in this lab to modify nanofibers, has been sintering. Sintering is the slow densification of material via diffusion-based minimization of surface area and may be used to achieve control of the resulting porosity. For example, Figure 6 shows electrospun polycaprolactone (PCL) that has been fully sintered to form a dense PCL membrane.

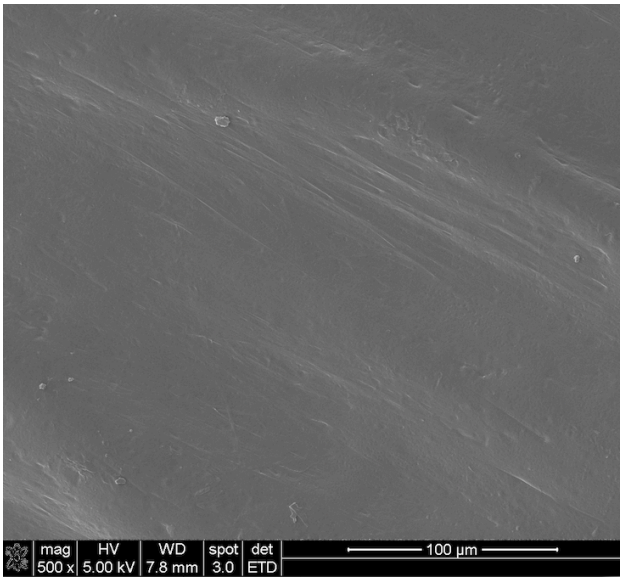

Figure 6. Scanning electron microscope image of fully sintered, electrospun PCL.

Electrospun PCL is a common choice for biomedical applications, and has been used repeatedly in electrospinning. This thermoplastic can be easily modified and combined with a number of other organic and inorganic polymers. PCL is considered biodegradable but degrades slowly so that the byproducts (e.g., caproic acid[14]) never reach lethal concentrations. For these reasons, PCL has been used in a number of drug release studies previously[15,16]. It has been polymerized with: drug throughout the material so that it releases this payload as it degrades, or drug and varying ratios of other polymers to control its degradation rate. PCL has also been used to create drug-

carrying matrices and drug-carrying disks, which release via diffusion through the polymer.

PCL is hydrophobic, and has a relatively simple backbone (Figure 7). These hydrophobic properties complicate PCL's interactions with aqueous environments, especially with fluids *in vivo*. For example, cell, protein, and enzyme adhesion to polymers depends heavily on polymer hydrophobicity, which can impact degradation, drug release, and drug metabolism.

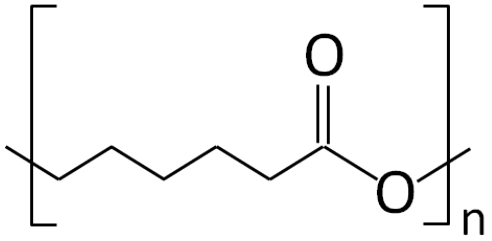

Figure 7. Polycaprolactone polymeric backbone.

To better understand how a fully sintered, electrospun layer of the proposed drug-eluting device will impact overall drug release, this paper focuses on characterizing the release mechanisms of this layer *in vitro.* A simplified approach may elucidate the major impacting factors for release, which will allow a better approach for modeling these systems in future studies and predicting the long-term device performance.

Materials and Methods

A. Sample Preparation

A PCL electrospinning stock solution of 5 wt% PCL dissolved in 1,1,1,3,3,3-hexoflouro-2-propanol (HFP) was prepared. 2 g of PCL was added to 38 g of HFP in a 100 mL narrow mouth glass beaker and stirred with a stir plate and stir rod at 40°C until dissolution occurred. The solution was transferred to a 60cc plastic syringe. The collector, a 3 mm diameter 316 stainless steel rod, with a length of 6 cm, was cleaned with 70% ethanol. The collector was held in a chuck of a corded electric drill and was set to rotate at the slowest drill setting, about 900 rpm. The rod was connected to ground by a small folded aluminum foil sheet, which allowed the rod to rotate freely while maintaining contact and connecting it to ground. The electrospinning was performed in a hood, using a 23 kV power supply, a syringe pump, and a 20 gauge needle tip to deliver the polymer solution at a flow rate of 5 mL/h to the collector, 20 cm away. Electrospinning was stopped at 12 minutes, when the desired capsule wall thickness of 500-700 μm was achieved. Thickness was measured on a Keyence Laser Micrometer. The resulting capsule thicknesses at the end of electrospinning are listed in Table 2.

Table 2. Thickness of the as-spun PCL nanofiber on the collecting rod.

Sample	Average Nanofiber Thickness (μm)
1	655
2	640
3	663
4	767

Porosity was decreased by sintering the as-spun sample. For this, all rods with the spun samples were placed inside a watertight plastic bag with all its air removed. This was

then placed in a water bath at 59°C for 3 hours. Cylindrical capsule samples approximately 1.5 cm long were then cut from the metal rod, and each sintered PCL sample thickness was recorded as it was removed from the rod. The average resulting sintered sample thickness was 143.3 ± 34.3 μm.

B. Sample Loading

In order to obtain a closed capsule to hold a drug reservoir inside, the cylindrical shaped sintered sample had to be sealed in both open areas. For this, one side of the capsule was sealed using a heat compression commercial sealer. The commercial sealer did not have direct temperature control, only a numeric heat scale. After investigation, it was found that the 2.5 setting could be used to seal PCL without adverse damage, so this was the setting used for sealing. A 10 mg/mL Rose Bengal stock solution in distilled water was made (Figure 8). From this, 20 μL were added to each capsule and the remaining open end was sealed using the same method, completely closing the capsule. The completed sample was then placed in a 10 mL glass vial with either distilled water or 1X phosphate buffered saline (PBS) and placed in an incubator at 37°C. The sample size for each condition was set to n = 5. An example of the resulting capsule setup is shown in Figure 9.

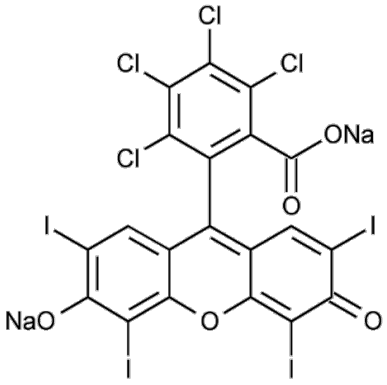

Figure 8. Rose Bengal molecule.

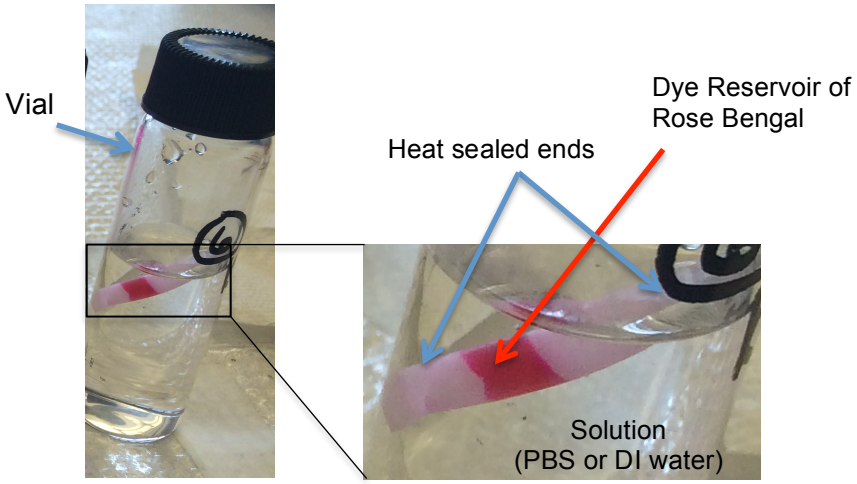

Figure 9. Sample setup example.

C. Release Analysis

A 100 µL aliquot of the test solution was transferred from each sample to a 96 well plate at specific times. A record of sample collection is shown in Appendix 1. The concentration of Rose Bengal at each time point was found by measuring the 96 well plate in a micro-plate reader (SpectraMax, M5 (Molecular Devices)). The micro-plate reader, using the setting of 540 nm excitation wavelength and 575 nm emissions wavelength, gave a value of fluorescent reading that was correlated to concentration using a pre-made calibration curve for Rose Bengal. In order to analyze the dye release over time on each specific media, a calibration curve was made for each one, PBS and distilled water. Both calibration curves were made in the range of 0 to 10 µg/mL.

Results and Discussion

A. Release Results

Figure 10 shows the release data for samples in distilled water and PBS, respectively. The figure shows the PBS solution elucidated a higher percentage of release over time. To investigate this significance, the average flux for each profile was calculated and compared.

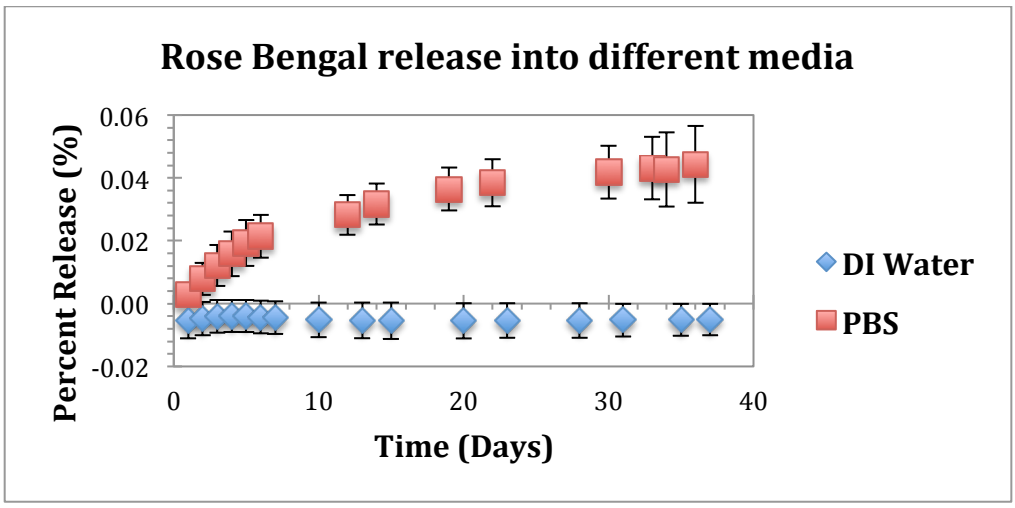

Figure 10. Percent release of Rose Bengal in 1X PBS solution and DI water.

Figure 11 shows the average flux for each condition calculated from the release data. A student's t-test comparing the calculated average flux of each solution resulted in a p-value of 0.001.

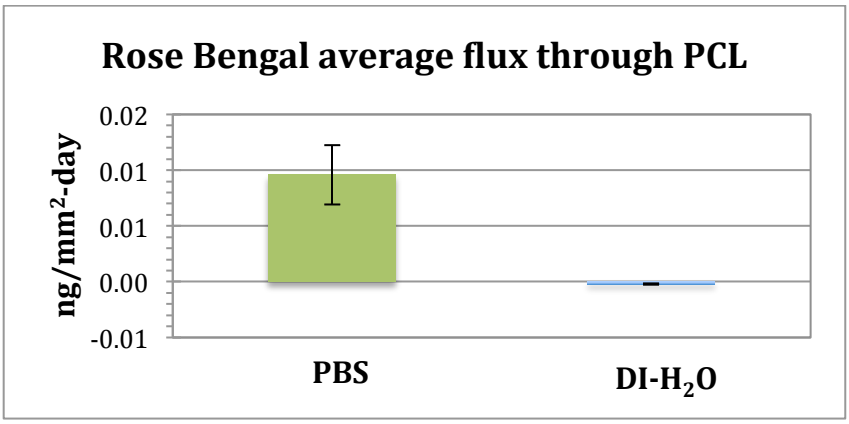

Figure 11. The average flux of Rose Bengal release through PCL.

B. Weight Gain Results Comparison

As verification for the results obtained in the release study, the results of another experimental setup are presented here. A weight gain study was conducted to test the performance of fully sintered electrospun PCL on a variety of different solution gradients.

The performance measure was capsule weight gain or loss over time. The results are shown in Figure 12. The figure shows that the capsule with PBS (inside of a capsule) and distilled water (outside of a capsule) had a significant weight gain. The results supported the results of this study, because in both studies, there was a detectable flux of mass when the PCL layer was between distilled water and PBS. In addition, the direction of flux was the same in both studies, as in the study mass flux was toward the PBS (indicated by weight gain) in the weight gain study and the dye flux was toward the PBS (out of the capsule and into the surrounding solution) in the release study.

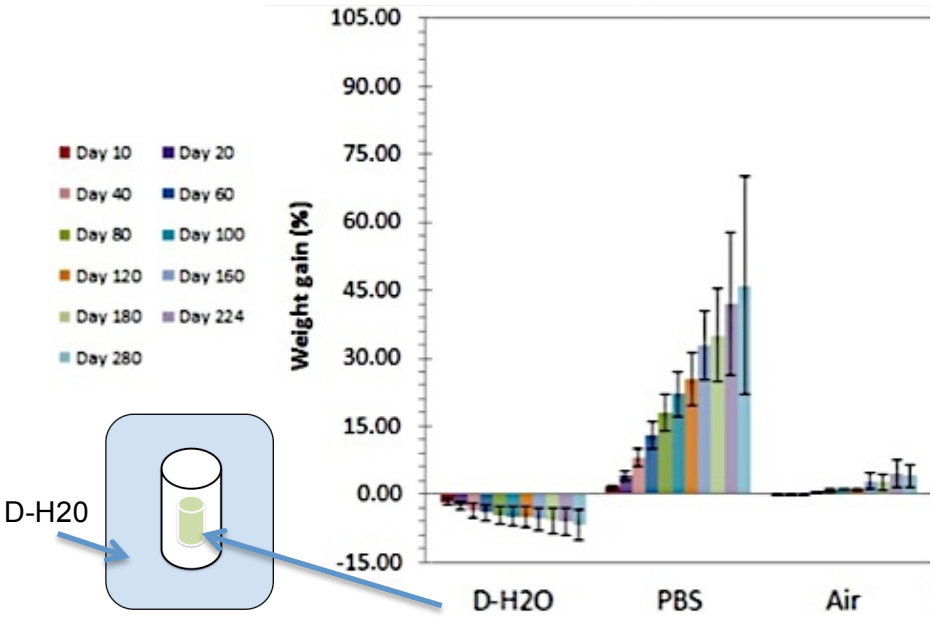

Figure 12. Weight gain study results.

C. Discussion

The PBS solution consists of ions, which are used to represent ion concentrations *in vivo*. The PBS solution had a working concentration of 137 mM NaCl, 2.7 mM KCl, 8 mM Na_2HPO_4 and 0.02% wt sodium azide. Also, the concentration of Rose Bengal in the reservoir was just 0.02 mM, comparatively. The high concentration of ions in solution could be impacting: the surface morphology of the PCL capsule, degradation, swelling, or wettability of the PCL capsule. In addition, the presence of ions introduces an osmotic pressure difference and could potentially be introducing an electronic charge gradient between the inside and outside of the capsule.

Surface morphology can be impacted by ions because ions are likely to be adhering to the PCL capsule surface as a result of the hydrophobicity of PCL. One published study tested release from PCL and poly(acrylic acid) (PAA) blends in PBS and simulated body

fluid (SBF)[14]. The study collected FTIR, SEM, and other surface measurements over a period of exposure time[14]. The results showed that solutions such as SBF and PBS can impact the surface and morphology of PCL composites, which intern may impact release. Furthermore, similar investigations of electrospun PCL and poly (D,L-lactic-co-glycolic) acid (PLGA) scaffolds have related mechanical properties and surface characteristics to drug release[15]. In both of these studies, the release was engineered to be degradation controlled, as drug was integrated throughout the polymer[14,15].

In contrast, experimental setups here may not be impacted by degradation of the PCL. Here, only PCL was used (not a blend), and compared to the time scale required for PCL degradation (about 2 years), differences in degradation rates between the two solution types may not be a likely cause of the difference in the release results which were only over a short time period (about 30 days), but this could be contributing the differences seen in the weight gain results (about 200 days)[17]. To further understand the basic potential mechanisms of release, a literature review was conducted to record the current modeling and predictive methods used in drug release studies.

D. Literature Review of Drug Release Modeling

The literature has attributed release from PCL to many different factors which creates challenges to predicting its behavior. The driving flux can be simplified into the following contributors: diffusion, pressure, electric potential, and temperature differences. These can be further rationalized to simplify the problem more. Temperature differences will be considered insignificant for the purposes of this investigation because both the device and the surrounding solution were maintained at 37°C within an incubator. Any electric potential present would be impacted by molecular charges of the solvent and solution

ions, and could theoretically be impacted by residual charge on the PCL from the electrospinning process. However, the sintering process likely allows any residual surface charge build-up to be relaxed. Pressure differences could also arise, due to ions in solution or device swelling, contributing to the mass flux.

Diffusion due to the reservoir concentration gradient has been the primary approach to modeling release in these experiments in the past. These are: based on Fick's first law, a constitutive equation which describes steady-state diffusion driven flux, (Equation 1); where D is the binary diffusion coefficient of the dilute solute in the solvent and $\frac{dC}{dx}$ is the solute concentration gradient:

(1) $$J_{diff} = -D * \frac{dC}{dx}$$

and based on Fick's second law, a description of the rate of concentration accumulation, (Equation 2); where $\frac{\partial C}{\partial t}$ is the change in concentration with respect to time.

(2) $$\frac{\partial C}{\partial t} = D * \frac{\partial^2 C}{\partial x^2}$$

From these, a number of equations based on flux by diffusion can be derived.
One notable equation is the Higuchi model, which predicts Fickian diffusion through a layer of ointment with drug placed on the skin surface. The key assumptions for the classical model are: the initial concentration, c_i, is much greater than the solute solubility, c_s, the drug diffusion in the ointment is the rate limiting step, the skin layer is a "perfect sink", and the ointment does not swell or dissolve during the release [18]. The result is Equation 3; where M_t is the cumulative amount of solute release per unit surface area, A, at time, t.

(3) $$\frac{M_t}{A} = \sqrt{2 c_i D c_s t}$$

This is a simple method for modeling the amount of drug release over time, however, the assumptions were also about a simple model, one-dimensional release through a homogeneous, thin slab. For one-dimensional release through polymeric slabs, a general solution to Fick's second law may be used. There are a number of general solutions, which vary in complexity depending on assumptions about: polymer matrix geometry, concentration dependent diffusivity, $D(c)$, boundary conditions, and matrix swelling [18]. Under the appropriate assumptions, one-dimensional diffusion analysis can also be expanded to uniform shapes such as cylinders and spheres by selecting the appropriate coordinate system and boundary systems.

In the past, pressure gradient has also been harnessed to control drug release. In these systems, osmotic pressure due to differences in solute concentrations cause a flexible reservoir or membrane to expand within a confined volume, creating a pressure that then delivers drug through a small orifice[19]. Examples of some of these devices are shown in Figure 13. In each of these examples, there is: a flexible membrane, separating an osmotic pressure gradient, which allows the flux of water to change the volume of the drug reservoir, pushing drug out through on orifice (Figure 13-A,B,C) or porous walls (Figure 13-D). Equations for modeling this type of drug delivery depend greatly upon the pressure gradient created. There are a number of equations derived for these systems based on differing geometries. As an example, a simple model is described in Equation 4; where $\frac{dV}{dt}$ is the differential volume element of water flowing into the osmotic membrane chamber over time[19].

(4) $$\frac{dM_t}{dt} = \left(\frac{dV}{dt}\right) * c_s$$

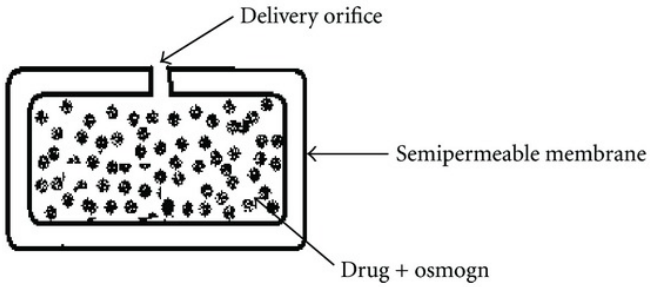

A. Elementary osmotic pressure pump delivery design.

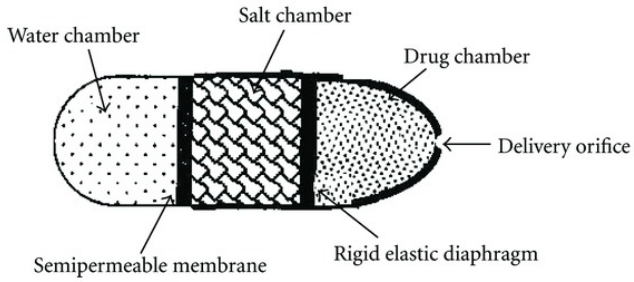

B. Rose Nelson osmotic pressure pump.

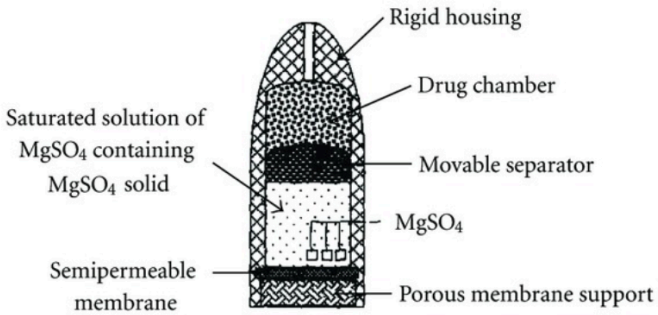

C. Higuchi-Leeper osmotic pressure pump design.

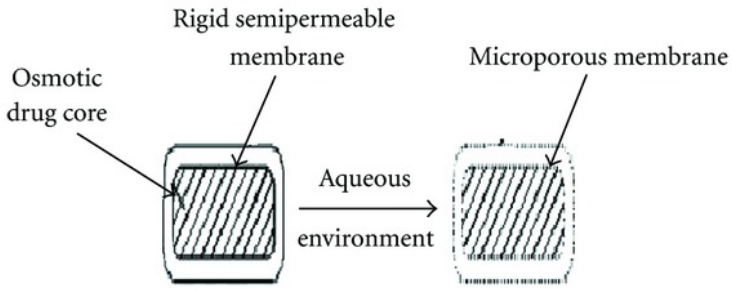

D. Controlled porosity osmotic pressure pump design.

Figure 13. Osmotic pressure pump designs and examples[19].

In systems of release through porous and nanoporous materials, D is often replaced with D_{eff}, or the effective diffusion coefficient, which takes into account factors such as: the volume fraction of space available for diffusion relative to the volume of the porous system, pore size, pore interconnectivity, the ratio of solute velocity to solvent velocity known as the retardation coefficient, or solute dispersion. And previously, transport through matrices has been modeled with varying complexity, from using Darcy's Law or Ritger-Peppas model[20], to much more complicated expansions of Fick's first and second laws[21].

In many approximations, the beginning (first 60%) of the release profile is modeled separately than the long-term release profile, because the beginning of release can show a "burst release" profile. This profile has been attributed to: surface concentrations of solute, uneven distribution of solute within a polymer, and more. However, this part of the release has historically been studied less thoroughly[22].

Conclusions

In conclusion, PBS significantly impacts the mechanisms governing release through the PCL capsule wall. This conclusion is reached by examining the release results, weight gain, an FTIR study, and finally the evidence of the many models predicting drug release behavior that specifically harness salt gradients created *in vivo*. These results are relevant to successfully modeling and predicting the long-term release of the proposed drug-delivering capsule. As such, the significant factors contributing to the release must be understood. Conversely, with a stronger fundamental understanding of the release mechanisms, higher performance devices may be targeted.

Future Studies

Eventually, future studies will include the creation of models that predict long-term capsule behavior. The information presented here will ultimately aid in determining which models and assumptions to choose, by helping to determine the true mechanisms of release. To further simplify the problem, and determine why the PCL is responding to exposure to PBS, future studies could investigate the change in the capsule's hydrophobicity over time, using contact angle and a goniometer. This would help to determine if a change in hydrophobicity at the surface is occurring, and if it is a change across a short or long timescale, therefore, impacting long-term, or only the short-term release.

Even though the results presented here support that flux is impacted by PBS regardless of which side of the membrane it is exposed to (inside or outside of the capsule), it would be valuable to determine the extent of osmotic pressure differences that could cause changes in the geometry of membrane, such as swelling which could expand either existing pores or polymer-chain spacing and increase the rate of release. This could potentially be investigated by comparing high-resolution electron microscopy images of capsules after exposure to solutions of varying salinity.

Future investigations will also include continued *in vitro* and *in vivo* studies involving Deslorelin. The drug can undergo hydrolysis (slowly), so the design of the *in vivo* studies requires the Deslorelin to be suspended in oil. This means that the ultimate device must have a solution gradient between the inside and outside of the capsule. Therefore, understanding the differences found in the release setup used here, a difference

between the inside (distilled water) and outside (PBS) is especially important, since the device will ultimately be subject to a solution gradient.

BIBLIOGRAPHY & REFERENCES

1 The Single-Rod Contraceptive Implant: History of Subdermal Contraceptive Implants. (2008).

2 Kutzler, M. & Wood, A. Non-surgical methods of contraception and sterilization. *Theriogenology* **66**, 514-525, doi:10.1016/j.theriogenology.2006.04.014 (2006).

3 Purswell, B. J. & Kolster, K. A. Immunocontraception in companion animals. *Theriogenology* **66**, 510-513, doi:10.1016/j.theriogenology.2006.04.018 (2006).

4 <http://www.michelsonprizeandgrants.org/home> (2017).

5 A review on polymer nanofibers by electrospinning and their applications in nanocomposites. **63**, 2223–2253, doi:10.1016/S0266-3538(03)00178-7 (2003).

6 *Introducing Electrospinning*, <http://electrospintech.com/slide4.html> (2017).

7 A comprehensive review summarizing the effect of electrospinning parameters and potential applications of nanofibers in biomedical and biotechnology. doi:10.1016/j.arabjc.2015.11.015 (2015).

8 Persano, L. *et al.* Industrial Upscaling of Electrospinning and Applications of Polymer Nanofibers: A Review. *Macromolecular Materials and Engineering* **298**, 504-520, doi:10.1002/mame.201200290 (2017).

9 *Nanofiber Solutions:: 3-D Cell Culture for a 3-D World*, <http://www.nanofibersolutions.com/> (2017).

10 Mataram, A. *et al.* WATER TREATMENT PERFOMANCE: APPLICATION OF ELECTROSPUN NANOFIBERS. *77*, doi:http://www.jurnalteknologi.utm.my/index.php/jurnalteknologi/article/view/5455 (2015).

11 Electrospun nanofibrous filtration membrane. **281**, 581–586, doi:10.1016/j.memsci.2006.04.026 (2006).

12 Nam, J., Huang, Y., Agarwal, S. & Lannutti, J. Improved Cellular Infiltration in Electrospun Fiber via Engineered Porosity. *Tissue Eng* **13**, 2249-2257, doi:10.1089/ten.2006.0306 (2007).

13 He, C., Nie, W. & Feng, W. Engineering of biomimetic nanofibrous matrices for drug delivery and tissue engineering. doi:10.1039/C4TB01464B (2014).

14 Mabrouk, M., Choonara, Y., Kumar, P., Toit, L. d. & Pillay, V. The Influence of Lyophilized EmuGel Silica Microspheres on the Physicomechanical Properties, In Vitro Bioactivity and Biodegradation of a Novel Ciprofloxacin-Loaded PCL/PAA Scaffold. *Polymers* **8**, 232, doi:10.3390/polym8060232 (2016).

15 Relationships between mechanical properties and drug release from electrospun fibers of PCL and PLGA blends. **65**, 724–733, doi:10.1016/j.jmbbm.2016.09.004 (2017).

16 Lam, C. X., Hutmacher, D. W., Schantz, J. T., Woodruff, M. A. & Teoh, S. H. Evaluation of polycaprolactone scaffold degradation for 6 months in vitro and in vivo. *J Biomed Mater Res A* **90**, 906-919, doi:10.1002/jbm.a.32052 (2009).

17 The return of a forgotten polymer—Polycaprolactone in the 21st century. **35**, 1217–1256, doi:10.1016/j.progpolymsci.2010.04.002 (2010).

18 Higuchi equation: Derivation, applications, use and misuse. **418**, 6–12, doi:10.1016/j.ijpharm.2011.03.051 (2011).

19 Keraliya, R. A. *et al.* Osmotic Drug Delivery System as a Part of Modified Release Dosage Form. *ISRN Pharm* **2012**, doi:10.5402/2012/528079 (2012).

20 Porta-i-Batalla, M. *et al.* in *Nanoscale Res Lett* Vol. 11 (2016).

21 Snyder, J. *et al.* An experimental and theoretical analysis of molecular separations by diffusion through ultrathin nanoporous membranes. *J Memb Sci* **369**, 119-129, doi:10.1016/j.memsci.2010.11.056 (2011).

22 Fu, Y. & Kao, W. J. Drug Release Kinetics and Transport Mechanisms of Non-degradable and Degradable Polymeric Delivery Systems. *Expert Opin Drug Deliv* **7**, 429-444, doi:10.1517/17425241003602259 (2010).

Appendices

Appendix 1. Sample Collection Record

Experiment:		20 uL of 10mg/ml Rose Bengal & Plain PLC in Distilled Water							
Time (All 2016)		Sample #	Place	Raw Data: Flourescent Reading					
1-Mar	15:30	0	A	-0.28025	1.37275	-0.24625	-0.42225	-0.33525	-0.32425
2-Mar	14:00	1	B	1.86775	72.1838	8.37475	6.10475	14.0078	2.79575
3-Mar	15:00	2	C	6.49375	88.1958	19.0928	16.7798	25.9918	7.43475
4-Mar	14:30	3	D	10.8218	96.0028	24.5708	27.0388	37.1498	15.8768
5-Mar	14:30	4	E	13.9698	93.6908	25.4958	31.9338	40.7908	15.4698
6-Mar	15:00	5	F	17.1978	86.2248	19.7288	30.9638	41.9408	13.9468
7-Mar	14:30	6	G	18.1778	79.3898	14.6528	23.5178	35.8878	11.7518
8-Mar	15:30	7	H	17.9588	65.8948	9.37375	21.2938	34.0718	11.5208
		0	A	-0.25109	-0.22309	-0.25109	-0.11609	-0.12609	-0.13309
11-Mar	15:00	8	B	10.3619	45.6079	4.16591	10.9239	19.0139	7.32991
14-Mar	14:30	9	C	11.2189	34.6599	4.29791	6.68791	13.3999	4.39091
16-Mar	15:30	10	D	7.45891	36.4249	4.21791	5.43091	9.80391	
21-Mar	15:30	11	E	2.76391	30.1879	4.64191	5.77391	12.3429	
24-Mar	12:38	12	F	2.85691		4.86791	5.56991	15.3239	
29-Mar	14:30	13	G	2.506		4.497	6.892	15.652	
1-Apr	14:30	14	H	2.833		3.951	7.51	22.998	
		0	A	-0.31856		-0.26756	-0.19556	-0.22756	
5-Apr	15:00	15	B	3.49544		4.18844	6.78144	27.3674	
7-Apr	16:00	16	C	3.29444		5.97044	8.18344	29.7474	
9-Apr	13:30	17	D	-0.44456		-0.27856	-0.27756	-0.30556	

		20 uL of 10mg/ml Rose Bengal & Plain PCL in PBS						
Time (All 2016)		Sample #	Place	Raw Data: Flourescent Reading				
2-Mar	14:00	0	A	-0.27209	-0.39209	-0.25109	-0.10209	0.09291
3-Mar	15:00	1	B	11.5009	74.9099	9.38191	108.245	30.5979
4-Mar	14:30	2	C	43.7609	143.084	44.3049	203.373	59.7499
5-Mar	14:30	3	D	66.3699	205.859	82.3819	258.449	94.1939
6-Mar	15:00	4	E	114.764	204.66	110.566	325.288	134.121
7-Mar	14:30	5	F	144.692	313.081	139.513	314.68	150.239
8-Mar	15:30	6	G	171.099	299.225	163.264	357.019	180.71
11-Mar	15:00	7	H	-0.32309	-0.13009	-0.04209	-0.01409	0.74791
		0	A	0.25091	0.03091	0.39591	0.23291	0.18991
14-Mar	14:30	8	B	244.991	378.138	241.099	409.504	239.792
16-Mar	15:30	9	C	33.2619	34.7729	33.5669	36.7249	36.5479
21-Mar	15:30	10	D	84.7159	79.1979	82.7459	78.4109	82.9749
24-Mar	12:38	11	E	103.042		110.879	96.7719	97.8289
29-Mar	14:30	12	F	-0.33109		0.29691	0.03591	0.08991
1-Apr	14:30	13	G	138.778		137.283	122.731	143.299
4-Apr	16:30	14	H	150.17		158.678	126.256	161.466
		0	A	0.25044		0.07144	0.39544	0.02544
5-Apr	15:00	15	B	144.951		152.278	119.254	163.089
7-Apr	16:00	16	C	17.1394		18.3834	10.0304	17.8354
9-Apr	13:30	17	D	-0.27556		-0.28756	-0.25756	-0.10956